Microwave Review
July 2024, Vol. 30, No. 1, pp. 81-86
DOI: 10.18485/mtts_mr.2024.30.1.11

A Compact High FOM UWB Planar Monopole Antenna Using Four Radiating Patch

Prasan Kumar Mishra, Tapan Kumar Patnaik, Bhavani Prasad Panda, Rabindra Kumar Mishra

Abstract –**This work presents a new compactly printed ultrawideband antenna for mobile satellites (8.025 GHz), metrological aids (9.5 GHz), and aeronautical radio navigation (9–9.2 GHz) applications. The proposed antenna is made up of four straightforward radiating rectangular-shaped strips, the overall geometry of which resembles two U-shaped in the radiating patch, fed by a 50Ω microstrip feed line. Two exponential patches, along with a rectangular patch, are implemented in the ground part of the structure, which can be effectively constructed by varying the sizes and geometries of these two U-shaped strips. The proposed antenna is compact overall. The proposed antenna is designed, simulated, fabricated, and tested minutely. The measured values of 10 dB return loss absolute/fractional BW of 10 GHz/142 % at the center frequency, minimum/maximum gain of 2/6.1 dBi, and maximum/minimum radiation efficiency of 92/70 % are achieved from the 2 to 12 GHz frequency range. These bandwidths are also well suited for 2.5/3.5/5.5-GHz WiMAX bands and 2.4/5.2/5.8-GHz WLAN bands. In addition, a comparison table is provided to prove the state-of-the-art design of the antenna.**

Keywords – **Compact; figure of merit (FOM); impedance bandwidth; improved gain; ultra-wideband (UWB).**

I. INTRODUCTION

Nowadays, researchers and the academic world have drastically surged in ultra-wideband (UWB) applications. In the meantime, the Federal Communication Commission (FCC) declared the frequency range of 3.1–10.6 GHz as an unlicensed band for the UWB in 2002. UWB-based antennas using different techniques, such as microstrip, multilayer, and substrate-integrated waveguide (SIW), have been reported in the literature. In this regard, some novel UWB antennas have been reported by researchers in [1]–[6]. The main advantages of a UWB antenna are that it provides a large channel capacity and the ability to work with a low signal-to-noise ratio. A UWB antenna has also offered many merits, such as low transmit power, superior penetration properties, jamming resistance, and high multipath channel performance.

However, UWB antennas exhibit multiple issues, like compact size, low gain, and efficiency. In order to overcome these issues, many authors have reported differently in other literature.

Article history: Received January 01, 2024; Accepted February 22, 2024.

P. K. Mishra, T. K. Patnaik, R. K. Mishra are with the GIET University, Gunupur, Odisha, India, E-mail: pkmishra@giet.edu, tapanpatnaik@giet.edu, and rabindramishra@giet.edu.

Bhavani Prasad Pand is with the Dept. of Physics, Chikiti Mohavidlaya, Chikiti, Chikiti, India, E-mail: nulu22@yahoo.com.

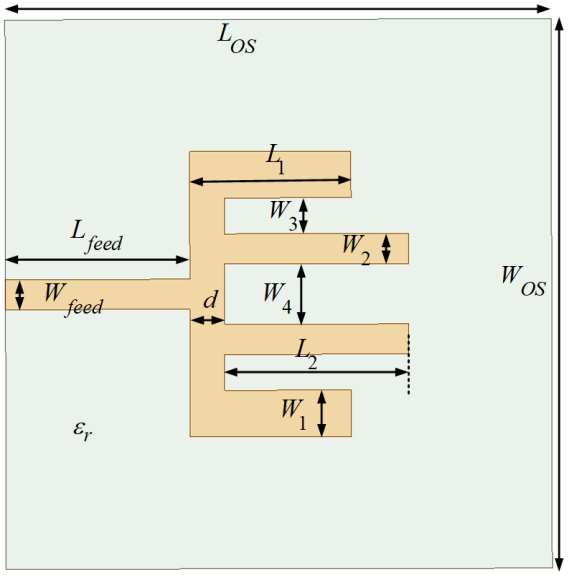

Fig. 1. Top view of proposed UWB antenna

In [7], using the antenna structure's magnetic coupling method, the symmetrical arrangement of the antenna structure has been designed in its compact UWB antenna. A dual-layer compact UWB antenna was also designed in order to make it small. The authors have implemented a circular cut on the radiation patch in [8] to enhance its antenna characteristics. In contrast, a Koch-fractal slot has been used on the antenna structure's radiation part [9]. As a result, the antenna size has been reduced to 70% of the surface compared to the original structure described in [10]. Again, to design a small UWB antenna, a rectangular aperture on the ground plane and a T-shape stub have been implemented in the designed structure, as reported in [11]. In order to reduce dimension and improve the antenna's impedance bandwidth, quasi-circular-shaped patches and triangle and tangent circle patches have been etched on the monopole antenna [12]. In [13], the UWB antenna structure has been used as a simple co-planar waveguide (CPW) feed. However, a half-annular ring has been etched on both sides of the radiator to alleviate the antenna's overall dimension. Two trapezoidal shapes were placed beside the feed to act as a ground for matching purposes [14]. On the other hand, a hollow elliptical shape is etched on top of the monopole and behaves like a good radiator. A trapezoidal-shaped patch has been placed on top of the monopole to improve radiation characteristics significantly and reduce the structure's size, as mentioned in [15]. Simultaneously, the two quasi-circular monopoles with rectangular ground have been implemented to obtain a high UWB performance.

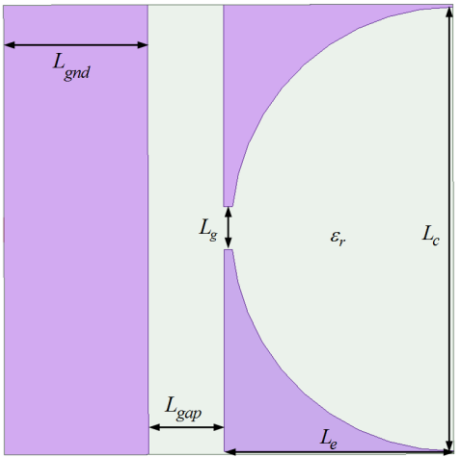

Fig. 2. Geometric and bottom view of proposed UWB antenna

In [16], by adding an inverted U-shape slot on the top of the monopole tapered radiator, which has been provided, the small size, UWB, and band rejection characteristics have been obtained. Nevertheless, many authors have also reported a compact size by using different techniques [17]-[21]. A compact and low-profile antenna for the use of folded ground plane [17], two inverted L-shape ground strips were placed at two opposite corners [18], microstrip to CPW strip-line Balun [19], folded-fin tapered [20], bending feed line structure in antipodal Vivaldi [21], and many more. Recently, the use of a circular ring along with an inverted L-shape monopole antenna [22], rectangular plate [23], hexagonal-shape slot along with rectangular stub [24], tapper line with parasitic strips [25], and slotted circular patch and etched rectangular slot on the ground [26] have been reported in the literature. Furthermore, a few UWB antennas have been designed and tested for compact size in [27]-[31]. In addition, a quad-port UWB MIMO antenna [34], a textile UWB antenna for healthcare monitoring [35], and a halved Vivaldi UWB antenna have recently been discussed.

Considering the above defects, the present work is undertaken to provide a better quality UWB antenna for this research. This paper focuses more on compact size, enhanced gain, and improving the UWB antenna's impedance bandwidth using a simple design approach. The designed antenna's overall dimension is 23.7 mm x 23.7 mm, equivalent to $0.55\lambda_0$ x $0.55\lambda_0$ at the center frequency, where the λ_0 is the free space wavelength in this design. However, the designed antenna is very compact compared to the precedent-reported literature. The main issues of the UWB antennas are less compact, low figure of merit and low cross polarization level. In light of this, we are mainly projected towards the compact size and high figure of merit. This paper presents a single-layer planar compact with a high figure of merit (FOM) UWB monopole antenna for mobile satellites, metrological aid, aeronautical radio navigation, WiMAX, and WLAN applications. The proposed structure comprises four radiating elements and two exponential metallic-shaped curves on the ground plane, which are etched on the ground part and placed on the left and right arm of the bottom part. The designed antenna is simulated, fabricated, and tested in the laboratory. The experimental results are matching with the simulated value.

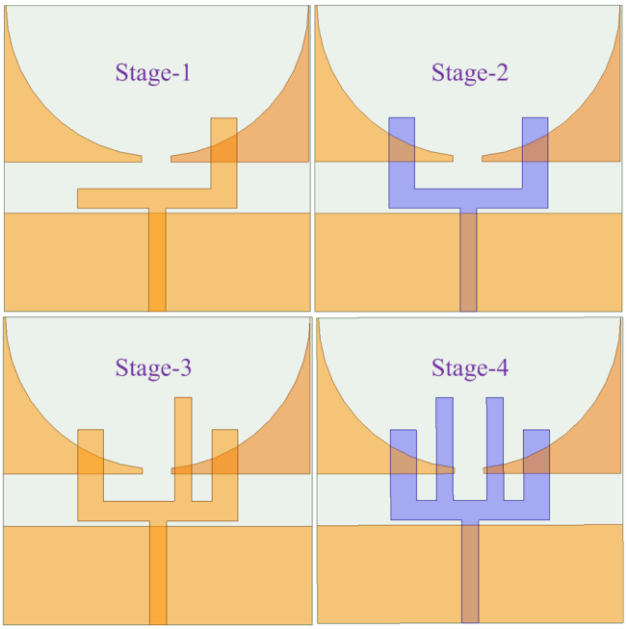

Fig. 3. Different stages of the proposed antenna

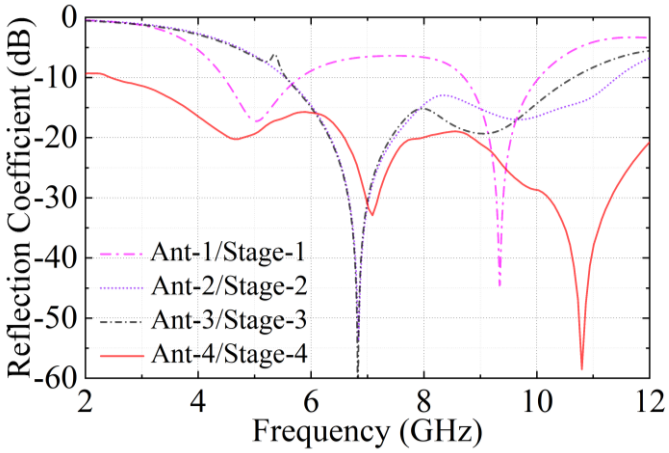

Fig. 4. Simulated results of reflection coefficient of the different stages of the proposed antenna

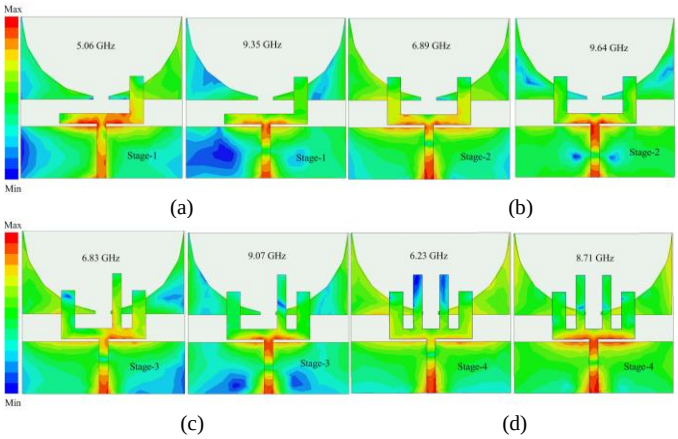

Fig. 5. Surface current distribution at the lower and higher frequencies: (a) Stage -1, (b) Stage-2, (c) Stage-3, (d) Stage-4

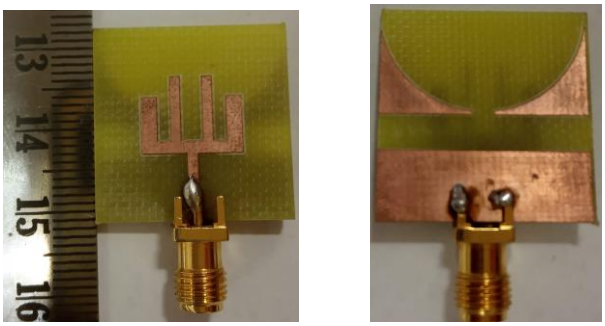

(a) (b)

Fig. 6. Laboratory prototype of the proposed antenna: (a) Top and (b) Bottom views

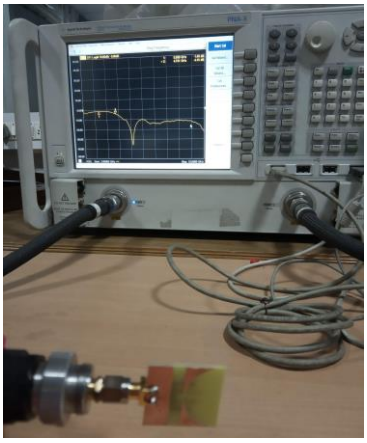

(a)

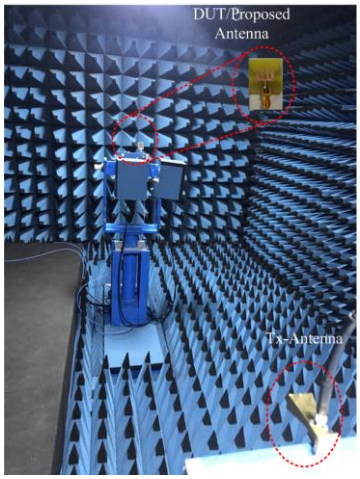

(b)

Fig. 7. Measurement setup of the proposed antenna: (a) VNA setup, (b) Anechoic chamber with DUT

II. Antenna Design

The antenna is optimized and simulated using the commercial electromagnetic software ANSYS HFSS ver. 17. The proposed antenna is designed with a FR4 substrate (23.7 x 23.7 x 1.6 mm^3) having a relative permittivity (ε_r) of 4.4 and loss tangent of 0.02. The proposed structure and its designed parameters are shown in Fig. 1 (a) and (b). This designed structure comprises four radiating elements and two exponential metallic-shaped curves on the ground plane, which are etched on the ground part and placed on the left and right arm of the bottom part. However, two exponential-shaped patches are printed, and a rectangular ground plane is on the dielectric substrate in the bottom part. In order to design the different stages of the structures and achieve the ultra-wideband, a simple patch antenna is created in the first stage, as shown in Fig. 2(a). Fig. 2 (b)-(d) depicts the rest of the structure. Fig. 2(a) shows the dimensions calculated to use the given mathematical expression in [32]. Meanwhile, the proposal's main objective is to obtain the antenna's UWB performance and good impedance matching.

The different stages of antenna structures improve performance, as shown in Fig. 2 and Fig. 3, respectively. It can be observed from Fig. 3 that the return losses are visualized as significantly improved in each stage of an antenna structure with a rectangular radiating stub's help. At the end, the dimensions of the design are fixed, as mentioned in the corresponding figures. Four rectangular radiating patches play a significant role in achieving a wider bandwidth, improving UWB performance. The first stage of the designed structure is shown in Fig. 3 (top corner left side). In this part, only one rectangular radiating patch is used. As a result, two resonant frequencies were obtained; one is around 5 GHz, and the other one is 9.3 GHz. It confirmed that the designed antenna did not cover the UWB band. The reflection coefficient vs. frequency plot is shown in Fig. 4. In the second stage (see Fig. 3 top right corner), another rectangular radiating patch is added along with an exciting radiating patch. It looks like a U-shape radiating patch. At the same time, the designed structure is simulated, and the 10 dB return loss is covered from 5.8-10.2 GHz, a frequency band that is not covered by the UWB band (3.1-10.6 GHz). Each radiating patch (or called stub) is approximately equal to a quarter wavelength ($\approx\lambda_g/4$=5.5 mm). At stage-3 (see Fig. 3 bottom left corner), another arm is added in the middle of the U-shape radiating patch. As a result, the UWB performance is a little bit improved, as shown in Fig. 4. In order to improve the UWB performance, another rectangular radiating patch is implemented between the U-shape patch and one radiating arm in the final stage (stage-4, see Fig. 3 right bottom corner). The design seems to be a combination of two U-shape radiating patches. In the meantime, the design is simulated, and as a result, the UWB performance is achieved at the end, as illustrated in Fig. 4.

In order to understand the creation of better radiation patterns in the UWB frequency bands, the current distribution at lower and higher frequencies are plotted, as depicted in Fig. 5. Finally, the optimized dimensions of the proposed work are listed below: W_{feed}=8.0, L_{feed}=1.3, L_1=7.0, L_2 =8.0, W_1=1.7, W_2=1.3, W_3=1.55, W_4 =2.6, L_{os}=23.7, W_{os}=23.7, L_c=23.7, L_g=2.25, L_{gap}=4, L_e=12.1, L_{gnd}=7.6, h=1.6 (unit: millimeters).

III. Simulation and Experimental Validation

The designed antenna is simulated with an Electromagnetic software Ansys HFSS 2020 R1. Then, it was fabricated and tested in the laboratory. The fabrication prototypes of the designed antenna are shown in Fig. 6. Performance was confirmed by fabricating and measuring the proposed antenna. Fig. 7 (a) shows the measurement setup with the vector

network analyzer (VNA). SMA connectors and an Agilent N5247A (10 MHz–67 GHz) vector network analyzer (VNA) are used in the experimental validation. In addition, experimental validation is used for the electronics calibration (Ecal) method. The VNA is notable for measuring the proposed antenna reflection coefficient. In the meantime, an anechoic chamber is used to measure the realized gain, radiation efficiency, and radiation patterns, as seen in Fig. 7(b).

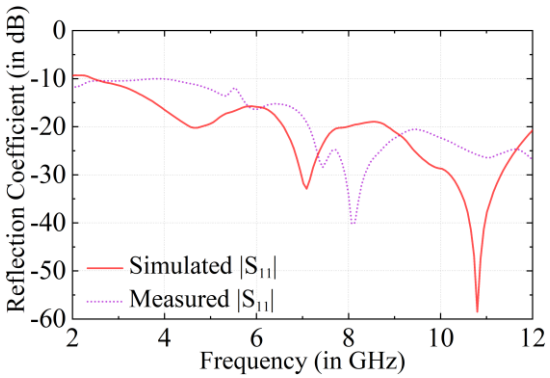

Fig. 8. Simulated and measured reflection coefficient of the proposed antenna

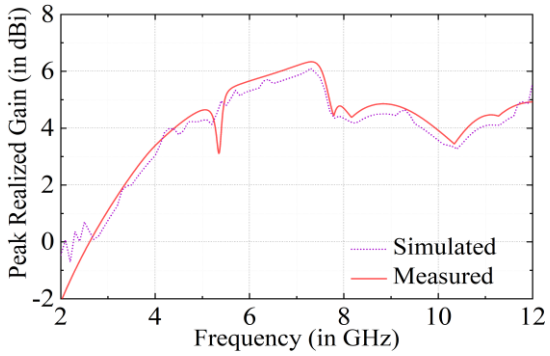

Fig. 9. Simulated and measured peak realized gain of the proposed antenna

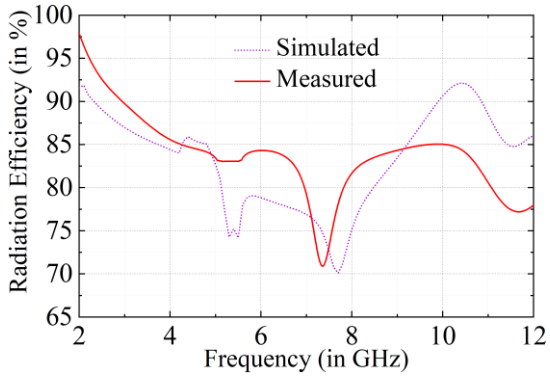

Fig. 10. Simulated and measured radiation efficiency of the proposed antenna

The simulated and experimental results of the reflection coefficient of the designed antenna are illustrated in Fig. 8. The measured two impedance bandwidths, -10 dB impedance absolute bandwidth (ABW) of 10 GHz (2–12 GHz), and -15 dB impedance ABW of 6.31 GHz (5.69–12 GHz), are achieved by the proposed fabricated antenna. In contrast, the simulated reflection coefficient of ABW of 10 GHz (2–12 GHz) and -15 dB impedance ABW of 6.31 GHz (5.69–12 GHz) are obtained. It also provides both simulated and measured fractional impedance bandwidth (FBW) of 142 % (-10 dB IBW) and impedance matching over the band. The simulated and measured gain of the antenna over the entire bandwidth is depicted in Fig. 9. It can be observed that the minimum-maximum range of measured peak realized gain of 2-6.1dBi (simulated: 2.02-6.33 dBi) are achieved. The Wheeler cap method is used to determine the reflection coefficient in free space. Then, a conductor encloses the antenna and the reflected power is transferred back to the feeding port under these circumstances. The radiated power is calculated by comparing the reflection coefficient in the free space [33].

TABLE 1

COMPARISON OF PRESENT WORK WITH THE STATE-OF-THE-ART

Ref.	Antenna Volume (λ_0^3)	Freq. (GHz)	Gain (dBi)	BW (%)	FOM
[27]	0.0399	3-11	-3.9 to 5.8	114	10565
[28]	0.0254	2.5-12.5	2 to 6.7	133	23195
[29]	0.0007	3-12	-4 to 5	NR	DI
[30]	0.0228	0.3-2	4.4 to 11.5	147	40214
[31]	0.0950	3-12	3.8 to 7.8	107/16	2692
[34]	0.2407	2-14	7.2	150	3240
[35]	0.0265	3-11	7.2	114	22541
[36]	0.0328	0.78-20	7.0	200	30487
This Work	**0.0112**	**2-12**	**2 to 6.1**	**142**	**51510**

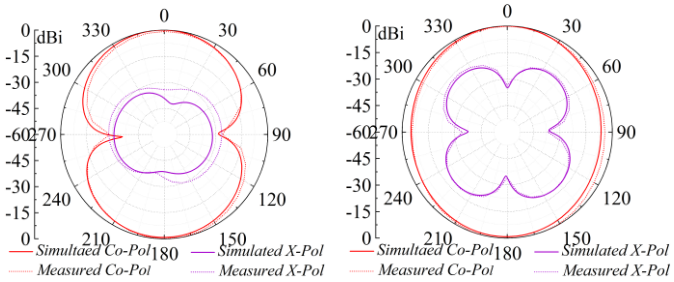

(a) (b)

Fig. 11. Normalized radiation patterns: (a) E-plane (XZ-plane) and (b) H-plane (YZ-plane) at 4.59GHz.

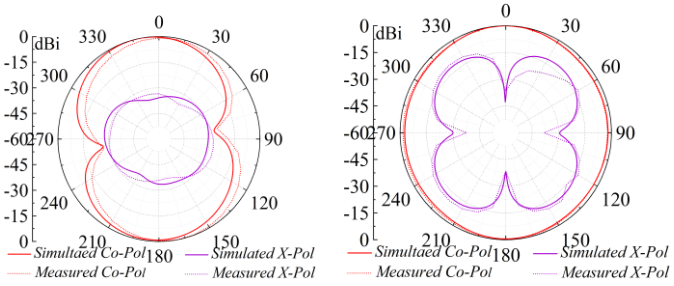

(a) (b)

Fig. 12. Normalized radiation patterns: (a) E-plane (XZ-plane), (b) H-plane (YZ-plane) at 4.59GHz.

$$\eta_m = 1 - \frac{P_{loss}}{P_{in}} = 1 - \frac{1 - |\Gamma_{wc}|^2}{1 - |\Gamma_{fc}|^2} = \frac{|\Gamma_{wc}|^2 - |\Gamma_{fc}|^2}{1 - |\Gamma_{fc}|^2} \quad (1)$$

The measured radiation efficiency is denoted by η_m, the Wheeler cap method's reflection coefficient is represented by $|\Gamma_{wc}|$ and the reflection coefficient in free space is represented by $|\Gamma_{fc}|$. From Fig. 10, it can be seen that the proposed design obtained the simulated maximum and minimum radiation efficiency of 95 and 71%, respectively, throughout the frequency band. In contrast, the measured maximum and minimum radiation efficiency of 92 and 70 % are achieved.

The simulated and experimental normalized radiation pattern at the two different frequencies of 17.08 and 24.55 GHz are plotted (E- and H-plane), as shown in Fig. 11. From these plots, it can be observed that the antenna exhibits an Omni-directional radiation pattern of E-plane. In the meantime, the antenna is also provided with an omnidirectional H-plane pattern. It is seen from Fig. 12(a) and (b) that the E- and H-plane provided a bidirectional pattern. The measured cross-polarization is lower than -34 dB for both E- and H-plane radiation patterns.

IV. Discussion

In addition, the FOM is introduced in this Section in order to add the fair comparison with our work. It is noted that the radiating patch increases with the decrease in resonant frequency. In light of this, the authors restricted the comparison of compact with reported in the lower or higher frequency range. However, the authors have introduced the figure of merit (FOM) in order to make a fair comparison with the reported previous work. The FOM is defined as:

$$FOM = \frac{Gain(\text{Absolute} - \text{scale}) \times \text{FBW}(\%)}{\frac{Volume}{\lambda_0^3}} \quad (2)$$

where FBW is the fractional bandwidth calculated at center frequency, Volume/λ_0^3 is the normalized transition volume (λ_0 is the operating wavelength at center frequency), and gain (peak realized gain) of the antenna (linear scale). Then, the FOM is calculated for each reported work and put in the Table 1. Finally, a comparison table is made to compare the similar types of UWB planar monopole antenna with the present work presented in Table I. The impedance bandwidth (FBW) is higher than [27]-[29], [31] and a little bit less than [30], [34], [36]. The peak realized gain is found to be higher than [27] and [29], [34], [36] and it is lower than [28], [30], [31]. It can be observed from Table I that the proposed antenna is more compact than [27]-[28],[30]-[31] and a little bit less compact than [29]. In order to make a fair comparison at the lower and higher frequencies, the FOM is introduced in this work. It is noted that the FOM is found to be better than the [27]-[31], [34], [36] except due to the data insufficient in [29], we are unable to calculate the FOM.

V. Conclusion

A single-layer planar compact with a high FOM UWB monopole antenna is presented for mobile satellites, metrological aid, and aeronautical radio navigation applications. This designed structure comprises four radiating elements and two exponential metallic-shaped curves on the ground plane, which are etched on the ground part and placed on the left and right arm of the bottom part. The designed antenna is fabricated and tested in the laboratory. The suitable impedance matching over the entire band from 2 to 12 GHz. The measured -10 dB impedance FBW is 142 % (ABW=10 GHz), the maximum gain is 6.1 dBi, and the maximum efficiency is 92 % over the band (2-12 GHz). These bandwidths are also well suited for 2.5/3.5/5.5-GHz WiMAX bands and 2.4/5.2/5.8-GHz WLAN bands.

Acknowledgement

The authors would like to thank the anonymous reviewers whose constructive comments have strengthened the article.

References

[1] A. K. Y. Lai, A. L. Sinopoli and W. D. Burnside, "A novel Antenna for Ultra-Wide-Band Applications", in *IEEE Transactions on Antennas and Propagation*, vol. 40, no. 7, pp. 755-760, July 1992.

[2] P. R. Clark and G. L. James, "Ultra-Wideband Hybrid-Mode Feeds", in *Electronics Letters*, vol. 31, no. 23, pp. 1968-1969, Nov. 1995.

[3] Symeon Nikolaou, G. E. Ponchak, J. Papapolymerou and M. M. Tentzeris, "Conformal Double Exponentially Tapered Slot Antenna (DETSA) on LCP for UWB Applications", in *IEEE Transactions on Antennas and Propagation*, vol. 54, no. 6, pp. 1663-1669, June 2006.

[4] Pengcheng Li, Jianxin Liang and Xiaodong Chen, "Study of Printed Elliptical/Circular Slot Antennas for Ultrawideband Applications", in *IEEE Transactions on Antennas and Propagation*, vol. 54, no. 6, pp. 1670-1675, June 2006.

[5] W. Lu and H. Zhu, "Design Concept of Compact Multilayer Ultra-Wideband Antipodal Slot Antenna", *IEEE Antennas and Propagation Society International Symposium*, Toronto, 2010, pp. 1-4.

[6] T. Jaschke, B. Rohrdantz, H. K. Mitto and A. F. Jacob, "Ultrawideband SIW-Fed Lens Antenna", in *IEEE Antennas and Wireless Propagation Letters*, vol. 16, pp. 2010-2013, 2017.

[7] N. Behdad and K. Sarabandi, "A compact antenna for ultrawide-band applications", in *IEEE Transactions on Antennas and Propagation*, vol. 53, no. 7, pp. 2185-2192, July 2005.

[8] B. Sanz-Izquierdo, P. R. Young, Q. Bai and J. C. Batchelor, "Compact UWB Monopole for Multilayer Applications", in *Electronics Letters*, vol. 42, no. 1, pp. 5-9, 5 Jan. 2006.

[9] W. J. Lui, C. H. Cheng and H. B. Zhu, "Compact Frequency Notched Ultra-Wideband Fractal Printed Slot Antenna", in *IEEE Microwave and Wireless Components Letters*, vol. 16, no. 4, pp. 224-226, April 2006.

[10] Seong-Youp Suh, W. L. Stutzman and W. A. Davis, "A New Ultrawideband Printed Monopole Antenna: the Planar Inverted cone Antenna (PICA) ", in *IEEE Transactions on Antennas and Propagation*, vol. 52, no. 5, pp. 1361-1364, May 2004.

[11] Y. Lin and K. Hung, "Compact Ultrawideband Rectangular Aperture Antenna and Band-Notched Designs", in *IEEE Transactions on Antennas and Propagation*, vol. 54, no. 11, pp. 3075-3081, Nov. 2006.

[12] Q. Wu, R. Jin, J. Geng and M. Ding, "Compact CPW-fed Quasi-Circular Monopole with Very Wide Bandwidth", in *Electronics Letters*, vol. 43, no. 2, pp. 69-70, 18 January 2007.

[13] H. K. Kan, W. S. T. Rowe and A. M. Abbosh, "Compact Coplanar Waveguide-fed Ultra-wideband Antenna", in *Electronics Letters*, vol. 43, no. 12, pp. 654-656, 7 June 2007.

[14] X. -. Yan, S. -. Zhong and G. -. Wang, "Compact Printed Monopole Antenna with 24:1 Impedance Bandwidth", in *Electronics Letters*, vol. 44, no. 2, pp. 73-74, 17 January 2008.

[15] Q. Wu, R. Jin and J. Geng, "Ultra-Wideband Quasi-Circular Monopole Antennas with Rectangular and Trapezoidal Grounds", in *IET Microwaves, Antennas & Propagation*, vol. 3, no. 1, pp. 55-61, February 2009.

[16] N. Mohammadian, M. -. Azarmanesh and S. Soltani, "Compact Ultra-Wideband Slot Antenna fed by Coplanar Waveguide and Microstrip Line with Triple-Band-Notched Frequency Function", in *IET Microwaves, Antennas & Propagation*, vol. 4, no. 11, pp. 1811-1817, November 2010.

[17] S. Kim and S. Nam, "Compact Ultrawideband Antenna on Folded Ground Plane", in *IEEE Transactions on Antennas and Propagation*, vol. 68, no. 10, pp. 7179-7183, Oct. 2020.

[18] J. Pourahmadazar and S. Mohammadi, "Compact Circularly-Polarised Slot Antenna for UWB Applications", in *Electronics Letters*, vol. 47, no. 15, pp. 837 -838, 21 July 2011.

[19] P. T. Nguyen, A. Abbosh and S. Crozier, "Wideband and Compact Quasi-Yagi Antenna Integrated with Balun of Microstrip to Slotline Transitions", in *Electronics Letters*, vol. 49, no. 2, pp. 88 -89, 17 January 2013.

[20] K. Kikuta and A. Hirose, "Compact Folded-Fin Tapered Slot Antenna for UWB Applications", in *IEEE Antennas and Wireless Propagation Letters*, vol. 14, pp. 1192-1195, 2015.

[21] G. K. Pandey, H. Verma and M. K. Meshram, "Compact Antipodal Vivaldi Antenna for UWB Applications", in *Electronics Letters*, vol. 51, no. 4, pp. 308-310, 19 2 2015.

[22] V. K. Sambhe, R. N. Awale and A. Wagh, "Compact Multi-band Novel-Shaped Planar Monopole Antenna for DCS, Bluetooth, and Ultra-Wide-Band Applications", in *The Journal of Engineering*, vol. 2016, no. 5, pp. 119-123, 2016.

[23] Q. Zhang and Y. Gao, "Compact low-profile UWB Antenna with Characteristic Mode Analysis for UHF TV White Space Devices", in *IET Microwaves, Antennas & Propagation*, vol. 11, no. 11, pp. 1629-1635, 2017.

[24] S. Saxena, B. K. Kanaujia, S. Dwari, S. Kumar and R. Tiwari, "Compact Ultra-Wideband Microstrip Antenna with Dual Polarisation/Multi-Notch Characteristics", in *IET Microwaves, Antennas & Propagation*, vol. 12, no. 9, pp. 1546-1553, 2018.

[25] T. Van Trinh and C. W. Jung, "Compact Broadband Internal Monopole Antenna with Parasitic Strips and Sleeve Feed for UHD-TV Applications", in *IET Microwaves, Antennas & Propagation*, vol. 13, no. 12, pp. 2096-2101, 2019.

[26] Q. Zhang and Y. Gao, "Compact low-profile UWB antenna with characteristic mode analysis for UHF TV white space devices", in *IET Microwaves, Antennas & Propagation*, vol. 11, no. 11, pp. 1629-1635, 2017.

[27] H. Huang, Y. Liu, S. Zhang, and S. Gong, "Uniplanar Differentially Driven Ultrawideband Polarization Diversity Antenna With Band-Notched Characteristics", *IEEE Antennas and Wireless Propagation Letters*, vol. 14, pp. 563–566, 2015.

[28] A. K. Nayak, D. Gountia, B. K. Turuk, and S. B. Panda, "Compact UWB Antenna for S, C, and X Bands Applications", in *2018 IEEE International Symposium on Smart Electronic Systems (iSES) (Formerly iNiS)*, 2018, pp. 183–186.

[29] L.-H. Ye and Q.-X. Chu, *Improved Band-notched UWB Slot Antenna*, Electronics Letters, vol. 45, pp. 1283–1285, December 2009.

[30] J. Guo, J. Tong, Q. Zhao, J. Jiao, J. Huo and C. Ma, "An Ultrawide Band Antipodal Vivaldi Antenna for Airborne GPR Application", in *IEEE Geoscience and Remote Sensing Letters*, vol. 16, no. 10, pp. 1560-1564, Oct. 2019.

[31] Y. Cheng and Y. Dong, "Ultra-Wideband Shared Aperture Crossed Tapered Slot Antenna for 5G Applications", in *IEEE Antennas and Wireless Propagation Letters*, pp. 1–5, 2022.

[32] A. K. Nayak, V. Singh Yadav and A. Patnaik, "Wideband Transition from Tapered Microstrip to Corrugated SIW", *IEEE MTT-S International Microwave and RF Conference (IMARC)*, Mumbai, India, 2019, pp. 1-4.

[33] A. K. Nayak, M. Chouhan, K. Moez, M. V. Kartikeyan and A. Patnaik, "Dual-Band Substrate Integrated Waveguide (SIW) Cavity Slot Antenna for C-Band Applications", *IEEE Microwaves, Antennas, and Propagation Conference (MAPCON)*, Bangalore, India, 2022, pp. 1302-1307.

[34] S. Javant, G. Srivastava and S. Kumar, "Quad-Port UWB MIMO Footwear Antenna for Wearable Applications", in *IEEE Transactions on Antennas and Propagation*, vol. 70, no. 9, pp. 7905-7913, Sept. 2022.

[35] S. Parameswari and C. Chitra, "Textile UWB Antenna with Metamaterial for Healthcare Monitoring", *Int. J. Antennas Propag.*, vol. 2021, 2021.

[36] B. Wu, X. -Y. Sun, H. -R. Zu, H. -H. Zhang and T. Su, "Transparent Ultrawideband Halved Coplanar Vivaldi Antenna With Metal Mesh Film", in *IEEE Antennas and Wireless Propagation Letters*, vol. 21, no. 12, pp. 2532-2536, Dec. 2022.